Journal of Magnetic Resonance **154,** 329–335 (2002)
doi:10.1006/jmre.2001.2489, available online at http://www.idealibrary.com on IDEAL®

COMMUNICATIONS

Using Conjoined Rigid Body/Torsion Angle Simulated Annealing to Determine the Relative Orientation of Covalently Linked Protein Domains from Dipolar Couplings

G. Marius Clore* and Carole A. Bewley†

*Laboratory of Chemical Physics, Building 5, National Institute of Diabetes and Digestive and Kidney Diseases, National Institutes of Health, Bethesda, Maryland 20892-0510; and †Laboratory of Bioorganic Chemistry, Building 8, National Institute of Diabetes and Digestive and Kidney Diseases, National Institutes of Health, Bethesda, Maryland 20892-0820

E-mail: clore@speck.niddk.nih.gov, caroleb@intra.niddk.nih.gov

Received September 17, 2001

A simple and robust method for determining the relative orientations of covalently linked protein domains using conjoined rigid body/torsion angle dynamics simulated annealing on the basis of residual dipolar couplings is presented. In this approach each domain is treated as a rigid body and the relevant degrees of conformational freedom are restricted to the backbone torsion angles (ϕ, ψ) of the linker between the domains. By this means translational information afforded by the presence of an intact linker is preserved. We illustrate this approach using the domain-swapped dimer of the HIV-inactivating protein cyanovirin-N as an example.

Residual dipolar couplings measured in a dilute liquid crystalline phase (*1–4*) provide unique long-range orientational information that is particularly valuable for defining relative orientations of structural elements in proteins and nucleic acids (*5–8*). Dipolar couplings can potentially lead to substantial improvements in coordinate accuracy for single domain proteins (*9–11*) and nucleic acids (*12–14*), particularly under conditions where other experimental NMR restraints are limited (*9, 11*). Perhaps one of the promising uses of dipolar couplings is in defining the relative orientations of individual components in protein–protein (*15–17*) and protein–nucleic acid (*18, 19*) complexes and the relative orientations of domains in multidomain proteins (*20–22*) and nucleic acids (*23*).

If the structures of the individual proteins of a complex are known at high accuracy in their free state (e.g., by crystallography) and conformational changes in the backbone upon complexation are insignificant, the simplest approach to determining the structure of a protein–protein complex on the basis of dipolar couplings and intermolecular NOE data involves the initial application of rigid body minimization (*16*), followed by conjoined rigid body/torsion angle (or cartesian coordinate) dynamics simulated annealing (*17, 24*). In this procedure, only the interfacial side chains are allowed to alter their conformation; the backbone and noninterfacial side chains of one protein are held fixed, while those of the second protein are only allowed to rotate and translate as a rigid body. To apply this approach or one involving a rigid body systematic grid search to a multidomain covalently linked system, it is necessary to sever the connection between the two domains (*20–22*). In doing so, translational information is lost and needs to be reintroduced either in the form of artificial distance restraints (*20*) or by only permitting hinge rotations of one domain relative to the other (*21, 22*). In this paper, we propose a simpler approach involving the application of a modified form of conjoined rigid body/torsion angle dynamics simulated annealing which preserves the linker between the two domains.

The modified conjoined rigid body/torsion angle dynamics simulated annealing approach that we propose is based on our recently described general internal variable dynamics module (IVM (*24*)) which has been incorporated into the program XPLOR-NIH (*25*). In internal coordinate dynamics, the molecule of interest is decomposed into collections of one or more atoms that are grouped together in rigid bodies referred to as clusters. Within a given cluster, the relative positions of the atoms are specified, and the clusters are connected by hinges that allow for motion of the clusters relative to one another (*24*). In conventional torsion angle dynamics, the clusters comprise groups of atoms whose geometry is fixed by covalent geometry and the hinges consist of torsion angles (i.e., for a protein, the backbone ϕ and ψ torsion angles and the side chain χ torsion angles). In this instance, however, each domain constitutes a cluster (i.e., a rigid body) and movement of one domain relative to the other occurs through rotation of backbone ϕ, ψ torsion angles within the linker connecting the two domains. Since the linkers are typically rather short, the number of degrees of freedom is

1090-7807/02

effectively limited to a very small number of torsion angles (two for each residue in the linker).

We illustrate this approach using the domain-swapped dimer of the HIV-inactivating protein cyanovirin-N (CVN) as an example. CVN occurs in two forms: a monomer whose structure has been solved by NMR (*10*) and a domain-swapped dimer solved by crystallography at low pH (*26*) and NMR at neutral pH (*20*). The structure of the monomer is identical to that of the AB′ (or A′B) half of the dimer (*26*), where A and A′ comprise residues 1–48 of each subunit and B and B′ comprise residues 55–101 of each subunit. Thus, in the domain-swapped dimer, residues 1–48 of one subunit and 55′–101′ of the other subunit correspond to the structure of the monomer (see Fig. 1). Following HPLC purification in organic solvent at low pH and subsequent lyophilization, CVN exists as an approximately 70 : 30 mixture of monomer and dimer (*20, 26*). Upon removal of organic solvent and raising the pH to neutral, most of the dimer is converted to monomer which represents ∼90% of the sample (*20, 26*). In previous work on such a mixed monomer/dimer sample (*20*) dissolved in a liquid crystalline medium of bicelles (*1*), $^1D_{NH}$ dipolar couplings could be measured for only 18 of 101 residues for the minor domain-swapped dimeric form (which is symmetric in solution), and it was shown that the relative orientation of the two halves of the dimer in solution differs by approximately 80–90° from that observed in the crystal structure. (The difference in orientation is due to a number of factors, including side chain electrostatic interactions and crystal packing (*20*).) The strategy employed (*20*) to determine the orientation of the domain-swapped dimer in solution involved the application of rigid body minimization (with the linker deleted and translational information provided by a small number of artifical distance restraints and a radius of gyration restraint) coupled with back-calculation of dipolar couplings on the basis of molecular shape (*27*) to distinguish the correct antiparallel solution from the incorrect parallel one.

For the present study the domain-swapped dimer at neutral pH was purified to homogeneity from a mixed monomer/dimer sample by gel filtration chromatography. The resulting pure dimer sample is stable at neutral pH and no interconversion to the monomeric form is observed. The availability of a pure dimeric sample enabled us to obtain a substantially larger number of dipolar couplings than was possible previously. $^1D_{NH}$ dipolar couplings for 68 of 101 residues (spanning residues 2–47 and 58–101) were measured in a polyethylene glycol

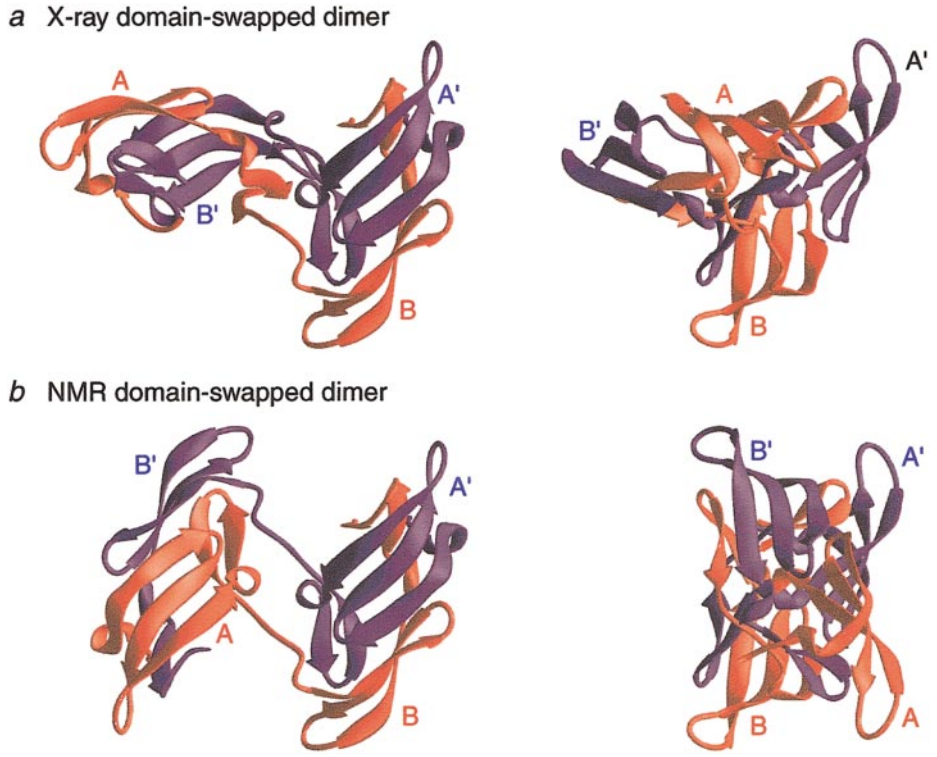

FIG. 1. Comparison of (a) the low pH X-ray structure (PDB accession code 3EZM (*26*)) and (b) the neutral pH NMR structure of the domain-swapped dimer of CVN. One subunit is shown in red and the other in blue. Each subunit is divided into N- and C-terminal portions: A and B, respectively, for the red subunit, and A′ and B′, respectively, for the blue subunit. The AB′ and A′B halves of the dimer are identical to the structure of the monomer solved by NMR. The minimal linker between the two halves of the domain-swapped dimer comprises residues 50–54 of one subunit and 50′–54′ of the other. The structures shown on the left-hand side of the figure share the same orientation of the A′B half of the domain-swapped dimer; likewise the two structures of the right-hand side of the figure share the same orientation of the A′B half of the domain-swapped dimer. A comparison of (a) and (b) clearly shows that the orientation of the AB′ half of the domain-swapped dimer relative to the A′B half differs by ∼80° in the X-ray and NMR structures.

(PEG (28))-based liquid crystalline medium (specifically a 5% $C_{12}E_5$ polyethylene glycol/hexanol mixture with a molar ratio of surfactant to alcohol of 0.96). Given the symmetric nature of the dimer, this corresponds to 136 (68×2) dipolar coupling restraints. A best fit of the alignment tensor using singular value decomposition (SVD (*27, 29*)) to the AB′ half of the X-ray coordinates (i.e., residues 1–48 of one subunit and 55′–101′ of the other which is equivalent to the monomer) yields a value of 14.1 Hz for the magnitude of the axial component of the alignment tensor (D_a^{NH}) and 0.65 for the rhombicity (η), with a dipolar coupling R factor (R_{dip} (*30*)) of 14.0% and a correlation coefficient of 0.97. The corresponding values of D_a^{NH} and η for the AB′ half of the domain-swapped dimer in the mixed monomer/dimer sample in a medium of 4.5% 3 : 1 DMPC : DHPC bicelles are 7.6 Hz and 0.21, with an R_{dip} of 13.6% and a correlation coefficient of 0.98. The overall difference in orientation of the alignment tensors in the PEG and bicelle liquid crystalline media is 18°.

Neither the dipolar couplings measured in PEG nor those measured in bicelles are consistent with the X-ray structure of the domain-swapped dimer and the values of R_{dip} obtained by SVD are 55.9 and 56.6%, respectively, with a correlation coefficient of ~0.6.

Two different protocols were employed to determine the relative orientation of the two halves of the domain-swapped dimer on the basis of the 68×2 dipolar coupling restraints measured in the PEG liquid crystalline medium.

In the first approach the X-ray structure (*26*) was used as the starting coordinates (Figs. 1a and 2a), and the calculations were carried out with five different linker lengths: residues 48–55, 49–55, 49–54, 50–55, and 50–54. The protocol comprises 78 cooling cycles, 0.3 ps in duration, of rigid body/torsion angle dynamics during which time the temperature is reduced from 1000 to 25 K in 12.5-K increments, followed by a few cycles of rigid body/torsion angle minimization. The force constant for the dipolar couplings (*31*) and for the noncrystallographic symmetry term (relating to the linker) is increased during cooling from 0.1 to 1.0 kcal · mol^{-1} · Hz^{-2} and from 1 to 100 kcal · mol^{-1} · Å^{-2}, respectively; while the force constants for the two terms representing the nonbonded contacts, namely the van der Waals repulsion term and the torsion angle conformational database term (*32*), were held constant at values of 4 kcal · mol^{-1} · rad^{-2} (with a van der Waals radius scale factor of 0.8) and 2, respectively. (Note that the purpose of the torsion angle conformational database term is to bias sampling during simulated annealing to conformations that are likely to be energetically possible by effectively limiting the choices of torsion angles to those that are known to be physically realizable (*32*).) Twenty structures each were calculated for each linker length, and the results are summarized in Fig. 2b and Table 1. The precision of each ensemble is high (~0.03 Å). The R_{dip} (work/PEG) for the working set of dipolar couplings measured in PEG and included in the refinement is ~14% (which is the same value as that obtained when best-fitting against only the A′B half of the dimer), and the cross-validated R_{dip} (free/bicelles) for the dipolar couplings measured in bicelles (which were not included in the calculations) is ~15–16% (Table 1). As is evident from Fig. 2b, the structures calculated with the different linker lengths are essentially indistinguishable: the pairwise backbone atomic rms displacement and rotation of the A′B half of the dimer for the five structure ensembles when best-fitting to the AB′ half ranged from 0.16 to 0.8 Å and from 0.3° to 2.1°, respectively. The corresponding values relative to the starting X-ray coordinates are ~20 Å and ~80°, respectively. Also provided in Table 1 are the values of the backbone ϕ/ψ torsion angles of the linkers in the different structures. The values of the ϕ/ψ torsion angles obtained for the different linker lengths are very similar and the differences reflect compensatory changes to accommodate the different numbers of torsion angles allowed to vary. In addition, it can be seen that the large difference in relative orientation of the two halves of the dimer observed in solution and in the X-ray structure arises principally from large changes from one highly favored region of the Ramachandran map to another in the ϕ angle of residue 53 and the ψ angles of residues 52 and 53. Thus the pivot point is centered around residues 52–53.

We also carried out a second set of calculations using the same protocol and starting coordinates (i.e., the X-ray structure) with the linker extending from residues 49–54 and the value of D_a^{NH} ranging from 12.1 to 16.1 Hz and η from 0.25 to 0.65. The rationale behind this set of calculations was to assess the impact of errors in the magnitude of the alignment tensor in the specific case of a dimer with C_2 symmetry. The largest difference in atomic rms displacement and orientation of the AB′ half of the domain-swapped dimer relative to the structure calculated with $D_a^{NH} = 14.1$ Hz and $\eta = 0.65$, with best-fitting to the A′B half, is ~1.2 Å and 5°, respectively, and is observed with the structures calculated with $D_a^{NH} = 16.1$ Hz and $\eta = 0.25$. Thus, in the case of C_2 symmetry, the results are relatively insensitive to the magnitude of the alignment tensor.

In the second approach, three different structures were generated by partially randomizing the ϕ, ψ angles of residues 49–54 subject to their lying in the allowed regions of the Ramachandran map by carrying out rigid body/torsion angle dynamics at 3000 K with no dipolar coupling restraints. The atomic and angular displacements of the AB′ half when best-fitting to the A′B half of the domain-swapped dimer ranged from 4–14 Å and 17–60°, respectively, relative to the X-ray structure, and from 21–25 Å and 85–112°, respectively, relative to the NMR structures calculated above. As a consequence of partial randomization of the ϕ, ψ angles of the linker, the path from the starting structures to the global minimum is rougher and more complex than that starting from the X-ray coordinates. Moreover, the measured dipolar couplings do not include any residues within the linker. Hence, a simulated annealing protocol with a larger radius of convergence is required. We therefore used our standared simulated annealing protocol for structure determination (*33*) with minor modifications to carry out conjoined rigid body/torsion angle dynamics in which the only degrees of freedom for the

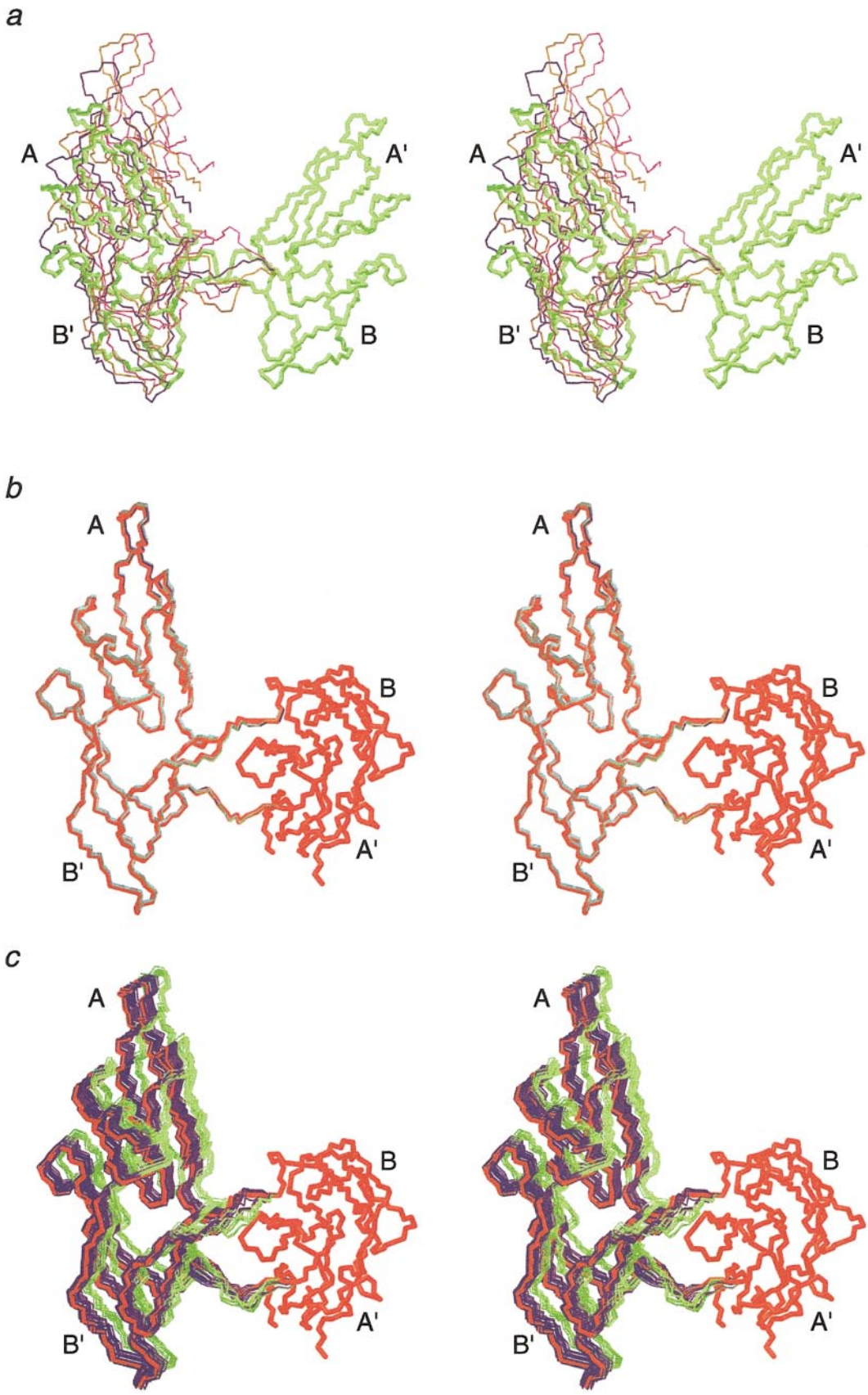
a
A
A'
B'
B
A
A'
B'
B
b
A
B
A'
B'
A
B
A'
B'
c
A
B
A'
B'
A
B
A'
B'

TABLE 1
Results of Conjoined Rigid Body/Torsion Angle Dynamics Based on Dipolar Couplings for the Domain-Swapped Dimer of CVN Using the First Protocol Starting from the X-Ray Coordinates[a]

		NMR Residues comprising linker				
	X-ray	48–55	49–55	49–54	50–55	50–54
Dipolar coupling *R* factor for dimer (%)[b]						
R_{dip} (work/PEG) (68 × 2)	55.9	14.0	14.1	14.2	14.2	14.3
R_{dip} (free/bicelles) (18 × 2)	56.6	15.7	15.6	15.3	15.6	15.3
Precision of backbone coordinate placement of the AB′ half when best-fitting to A′B half (Å)[c]	—	0.03	0.02	0.02	0.01	0.04
Backbone atomic rms displacement of AB′ half relative to X-ray with best-fitting to A′B half (Å)	0	20.2	20.2	20.0	20.1	20.0
Orientation of AB′ half relative to X-ray with best-fitting to A′B half (°)	0	80.8	80.8	80.0	79.6	78.8
ϕ/ψ torsion angles in linker (°)[d]						
K48	−130/155	−128/164	[e]	[e]	[e]	[e]
W49	−74/135	−78/153	−71/152	−70/153	[e]	[e]
Q50	−87/132	−135/158	−133/158	−134/159	−115/159	−117/160
P51	−65/138	−57/178	−55/176	−53/177	−50/176	−50/177
S52	−82/−3	−75/**175**	−68/**179**	−78/−**178**	−64/−**177**	− 63/−**170**
N53	−169/71	−**72**/−**146**	−**76**/−**141**	−**76**/−**167**	−**85**/−**134**	−**90**/−**138**
F54	−127/–10	−129/–31	−133/–51	−112/–34	−140/–57	−135/–41
I55	−75/–10	−68/–18	−56/–14	[e]	−53/–17	[e]

[a] The values reported in the table for the various parameters relating to the NMR structures refer to the average values for an ensemble of 20 structures calculated for each linker length. The PDB accession code for the X-ray structure (*26*) is 3EZM.

[b] The dipolar coupling *R* factor ($R_{dip}(30)$) is defined as the ratio of the rms deviation between observed and calculated values to the expected rms deviation if the vectors were randomly oriented. The latter is given by $\{2D_a^2[4+3\eta^2]/5\}^{1/2}$, where D_a is the magnitude of the axial component of the alignment tensor and η the rhombicity (*30*). The values of D_a^{NH} and η were obtained by a singular value decomposition best-fit procedure using the coordinates of the monomer (i.e., the AB′ half of the X-ray coordinates of the domain-swapped dimer). The values of D_a^{NH} and η in PEG (derived from 68 measured $^1D_{NH}$ couplings) are 14.1 Hz and 0.65, respectively, and the value of R_{dip} (monomer/PEG) for the monomer is 14.0%. The values of D_a^{NH} and η in bicelles (derived from 18 measured $^1D_{NH}$ couplings) are 7.6 Hz and 0.21, respectively, and the value of R_{dip} (monomer/bicelles) for the monomer is 13.6%. (For consistency with our previous publication on the domain-swapped dimer of CVN (*20*), the sign of the $^1D_{NH}$ dipolar couplings and hence the sign of D_a^{NH} take into account the fact that the $^1J_{NH}$ couplings are negative.) Note that the values of R_{dip} (free/bicelles) for the dimer reported in the table represent cross-validated values since they are *not* included in the calculation. The standard deviations of the reported R_{dip} (work/PEG) and R_{dip} (free/bicelles) values reported in the table are less than 0.1%.

[c] Precision in the placement of the A′B half of the domain-swapped dimer relative to the AB′ half is defined as the average atomic rms displacement between the individual structures and the mean coordinates when carrying out the best-fitting with respect to the A′B half of the domain-swapped dimer. Note that the AB′ and A′B halves of the domain-swapped dimer are treated as rigid bodies and the domain-swapped dimer is completely symmetric.

[d] The standard deviations in the torsion angles is less than 1° with the exception of the structures calculated with residues 48–55 as the linker between the two halves of the domain-swapped dimer. The standard deviations for the torsion angles for this ensemble of structures range from 1–5° with the exception of the ψ angles of K48 and N53, and the ϕ angles of W49, N53, and F54 which range from 7–25°.

[e] These torsion angles are held fixed at their values in the X-ray structure of the domain-swapped dimer.

FIG. 2. Results of rigid body/conjoined torsion angle dynamics based on dipolar couplings for the domain-swapped dimer of CVN. (a) Starting structures (backbone N, Cα, C′ atoms), best-fitted to the A′B half of the domain-swapped dimer of CVN used in the calculations with the X-ray structure represented by thick green lines, and three alternative starting structures shown as thin blue, gold, and purple lines, generated by partial randomization of the ϕ, ψ angles of the linker (residues 49–54) within the confines of the allowed regions of the Ramachadran map. (b) Structures, best-fitted to the A′B half of the domain-swapped dimer, generated by conjoined rigid body/torsion angle dynamics starting from the X-ray structure. The thick red line represents the ensemble of 20 structures generated with the ϕ/ψ torsion angles of residues 49–54 allowed to vary; the other 4 ensembles of structures (20 each) are represented by thin lines and were generated with the ϕ/ψ torsion angles of residues 48–55 (purple), 49–55 (blue), 50–55 (green), and 50–54 (cyan) allowed to vary. The five ensembles of structures are essentially indistiguishable from each other. (c) Structures, best-fitted to the A′B half of the domain-swapped dimer, generated by conjoined rigid body/torsion angle dynamics starting from the three alternate structures shown in (a). Two ensembles of structures were obtained, displayed in blue (35 structures) and green (25 structures) with the same orientation of the AB′ half the domain-swapped dimer relative to the A′B half but with different translational displacements; for comparison, the average structure of the red ensemble shown in (b) is also displayed (thick red line).

backbone are afforded by the ϕ, ψ torsion angles in the linker (residues 49–54). This protocol comprises (a) high temperature equilibration at 3000 K; (b) slow cooling during which time the force constants for the dipolar coupling restraints (obtained in PEG), the noncrystallographic symmetry term, and the conformational torsion angle database term are increased from 0.1 to 1 kcal $\cdot$ mol^{-1} $\cdot$ Hz^{-2}, 1 to 100 kcal $\cdot$ mol^{-1} $\cdot$ Å^{-2}, and 0.1 to 8, respectively; and (c) a few cycles of conjoined rigid body/torsion angle minimization. (Note that since there are no experimental restraints for the linker, a large final value for the force constant for the conformational torsion angle database term is employed to ensure that the ϕ, ψ angles for the linker reside within the preferred regions of the Ramachandran map.) The results are summarized in Fig. 2c. The resulting structures can be divided into two main groups in a ratio of $\sim 3:2$. The atomic rms displacement of the AB′ half of the domain-swapped dimer relative to that of the structures obtained starting from the X-ray coordinates when best-fitting to the A′B half is 0.8 ± 0.3 Å for the first group and 2.7 ± 0.1 Å for the second group. These displacements are entirely translational in nature, since the relative orientations of the two halves of the dimer are essentially identical for the calculated structures obtained from both protocols, differing by less than 2°. Both groups had the same R_{dip} (work/PEG) and R_{dip}(free/bicelles) values of 14.1 ± 0.1 and $15.6 \pm 2.3\%$, respectively.

The relative orientation of the AB′ and A′B halves in the solution structure of the domain-swapped dimer at neutral pH is ~120°, which we term the antiparallel solution (Figs. 1b, 2b, and 2c). An alternative solution with the two halves oriented at ~−60° (i.e., 180° relative to the first solution), which we term the parallel solution, is also potentially consistent with a single set of dipolar couplings (*20*). As discussed previously (*20*), the measured dipolar couplings in bicelles are completely inconsistent with the predicted dipolar couplings for the parallel solution calculated on the basis of shape using a steric obstruction model (*27*). A small number of structures (~10%), corresponding to the parallel solution, were obtained with the second calculational protocol. The R_{dip} (work/PEG) for these so-called parallel structures was $15.2 \pm 0.4\%$, slightly worse than that obtained for the antiparallel solution (~14%); however, the R_{dip}(free/bicelles) for the parallel structures was $35 \pm 1\%$ compared to 15–16% for the antiparallel structures. Thus, dipolar couplings measured in a second liquid crystalline medium can readily distinguish between the two alternate solutions.

In conclusion, we have presented a simple and robust approach using conjoined rigid body/torsion angle dynamics for determining the relative orientations of two domains (in this case the two-halves of a domain-swapped dimer) on the basis of dipolar couplings. Since the relevant conformational degrees of freedom are limited to the ϕ, ψ backbone torsion angles of the linker region between the two domains, the approach is highly efficient and displays excellent convergence properties while retaining translational information afforded by the presence of an intact linker.

ACKNOWLEDGMENTS

This work was supported in part by the AIDS Targeted Antiviral program of the Office of the Director of the National Institutes of Health. The coordinates for the NMR structure of the domain-swapped dimer of CVN at neutral pH have been deposited in the RCSB protein data bank (Accession code 1J4V).

REFERENCES

1. N. Tjandra and A. Bax, Direct measurement of distances and angles in biomolecules by NMR in a dilute liquid crystalline medium, *Science* **278,** 1111–1114 (1997).
2. G. M. Clore, M. R. Starich, and A. M. Gronenborn, Measurement of residual dipolar couplings of macromolecules aligned in the nematic phase of a colloidal suspension of rod-shaped viruses, *J. Am. Chem. Soc.* **120,** 10571–10572 (1998).
3. M. R. Hansen, L. Mueller, and A. Pardi, Tunable alignment of macromolecules by filamentous phage yields dipolar coupling interactions, *Nature Struct. Biol.* **5,** 1065–1074 (1998).
4. J. H. Prestegard, H. M. al-Hashimi, and J. R. Tolman, NMR structures of biomolecules using field oriented media and residual dipolar couplings, *Q. Rev. Biophys.* **33,** 371–424 (2000).
5. N. Tjandra, J. G. Omichinski, A. M. Gronenbron, G. M. Clore, and A. Bax, Use of dipolar ^{1}H-^{15}N and ^{1}H-^{13}C couplings in the structure determination of magnetically oriented macromolecules in solution, *Nature Struct. Biol.* **4,** 732–738 (1997).
6. C. A. Fowler, F. Tian, H. M. Al-Hashimi, and J. H. Prestegard, Rapid determination of protein folds using residual dipolar couplings, *J. Mol. Biol.* **304,** 447–460 (2000).
7. F. Delaglio, G. Kontaxis, and A. Bax, Protein structure determination using molecular fragment replacement and NMR dipolar couplings, *J. Am. Chem. Soc.* **122,** 2142–2143 (2000).
8. J. C. Hus, D. Marion, and M. Blackledge, Determination of protein backbone structure using only residual dipolar couplings, *J. Am. Chem. Soc.* **123,** 1541–1542 (2001).
9. G. M. Clore, M. R. Starich, C. A. Bewley, M. Cai, and J. Kuszewski, Impact of residual dipolar couplings on the accuracy of NMR structures determined from a minimal number of NOE restraints, *J. Am. Chem. Soc.* **121,** 6513–6514 (1999).
10. C. A. Bewley, K. R. Gustafson, M. R. Boyd, D. G. Covell, A. Bax, G. M. Clore, and A. M. Gronenborn, Solution structure of cyanovirin-N, a potent HIV-inactivating protein, *Nature Struct. Biol.* **5,** 571–578 (1998).
11. W.-Y. Choi, M. Tollinger, G. A. Mueller, and L. E. Kay, Direct structure refinement of high molecular weight proteins against residual dipolar couplings and carbonyl chemical shift changes upon alignment: An application to maltose binding protein, *J. Biomol. NMR* **21,** 31–40 (2001).
12. A. Vermeulen, H. Zhou, and A. Pardi, Determining DNA global structure and DNA bending by application of NMR residual dipolar couplings, *J. Am. Chem. Soc.* **122,** 9638–9647 (2000).
13. N. Tjandra, S. Tate, A. Ono, M. Kainosho, and A. Bax, The NMR structure of a DNA dodecamer in an aqueous dilute liquid crystalline phase, *J. Am. Chem. Soc.* **122,** 6190–6200 (2000).
14. J. Kuszewski, C. Schwieters, and G. M. Clore, Improving the accuracy of NMR structures of DNA by means of a database potential of mean force describing base-base positional interactions, *J. Am. Chem. Soc.* **123,** 3903–3918 (2001).

15. D. S. Garrett, Y.-J. Seok, A. Peterkofsky, A. M. Gronenborn, and G. M. Clore, Solution structure of the 40,000 Mr phosphoryl transfer complex between the N-terminal domain of enzyme I and HPr, *Nature Struct. Biol.* **6,** 166–173 (1999).
16. G. M. Clore, Accurate and rapid docking of protein-protein complexes on the basis of intermolecular nuclear Overhauser enhancement data and dipolar couplings by rigid body minimization, *Proc. Natl. Acad. Sci. U.S.A.* **97,** 9021–9025 (2000).
17. G. Wang, J. M. Louis, M. Sondej, Y.-J. Seok, A. Peterkofsky, and G. M. Clore, Solution structure of the phosphoryl transfer complex between the signal transducing proteins HPr and $IIA^{Glucose}$ of the *Escherichia coli* phosphoenolpyruvate : Sugar phosphotransferase system, *EMBO J.* **19,** 5635–5649 (2000).
18. K. Huang, J. M. Louis, L. Donaldson, F.-L. Lim, A. D. Sharrocks, and G. M. Clore, Solution structure of the MEF2A-DNA complex: Structural basis for the modulation of DNA bending and specificity by MADS-box transcription factors, *EMBO J.* **19,** 2615–2628 (2000).
19. E. C. Murphy, V. B. Zhurkin, J. M. Louis, G. Cornilescu, and G. M. Clore, Structural basis for SRY-dependent 46-X,Y sex reversal: Modulation of DNA bending by a naturally occuring point mutation, *J. Mol. Biol.* **312,** 481–499 (2001).
20. C. A. Bewley and G. M. Clore, Determination of the relative orientation of the two halves of the domain-swapped dimer of cyanovirin-N in solution using dipolar couplings and rigid body minimization, *J. Am. Chem. Soc.* **122,** 6009–6016 (2000).
21. N. R. Skrynnikov, N. K. Goto, D. Yang, W. Y. Choi, J. R. Tolman, G. A. Mueller, and L. E. Kay, Orienting domains in proteins using dipolar couplings measured by liquid-state NMR: Differences in solution and crystal forms of maltodextrin binding protein loaded with β-cyclodextrin, *J. Mol. Biol.* **295,** 1265–1273 (2000).
22. N. K. Goto, N. R. Skynnikov, F. W. Dalhquist, and L. E. Kay, What is the average conformation of bacteriophage T4 Lysozyme in solution? A domain orientation study using dipolar couplings measured by solution NMR, *J. Mol. Biol.* **308,** 745–764 (2001).
23. E. T. Mollova, M. R. Hansen, and A. Pardi, Global structure of RNA determined with residual dipolar couplings, *J. Am. Chem. Soc.* **122,** 11561–11562 (2000).
24. C. D. Schwieters and G. M. Clore, Internal coordinates for molecular dynamics and minimization in structure determination and refinement, *J. Magn. Reson.* **152,** 288–302 (2001).
25. G. M. Clore, J. Kuszewski, C. D. Schwieters, and N. Tjandra, XPLOR-NIH, available at http://nmr.cit.nih.gov/xplor-nih.
26. F. Yang, C. A. Bewley, J. M. Louis, K. R. Gustafson, M. R. Boyd, A. M. Gronenborn, G. M. Clore, and A. Wlodawer, Crystal structure of cyanovirin-N, a potent HIV-inactivating protein, shows unexpected domain swapping, *J. Mol. Biol.* **288,** 403–412 (1999).
27. M. Zweckstetter and A. Bax, Prediction of sterically induced alignment in a dilute liquid crystalline phase: Aid to protein structure determination by NMR, *J. Am. Chem. Soc.* **122,** 3791–3792 (2000).
28. M. Rückert and G. Otting, Alignment of biological macromolecules in novel nonionic liquid crystalline media for NMR experiments, *J. Am. Chem. Soc.* **122,** 7793–7797 (2000).
29. J. A. Losonczi, M. Andrec, M. W. Fischer, and J. H. Prestegard, Order matrix analysis of residual dipolar couplings using singular value decomposition, *J. Magn. Reson.* **138,** 334–342 (1999).
30. G. M. Clore and D. S. Garrett, R-factor, free R, and complete cross-validation for dipolar coupling refinement of NMR structures, *J. Am. Chem. Soc.* **121,** 9008–9012 (1999).
31. G. M. Clore, A. M. Gronenborn, and N. Tjandra, Direct structure refinement against residual dipolar couplings in the presence of rhombicity of unknown magnitude, *J. Magn. Reson.* **131,** 159–162 (1998).
32. J. Kuszewski and G. M. Clore, Source of and solutions to problems in the refinement of protein NMR structures against torsion angle potentials of mean force, *J. Magn. Reson.* **146,** 249–254 (2000).
33. J. G. Omichinski, P. V. Pedone, G. Felsenfeld, A. M. Gronenborn, and G. M. Clore, The solution structure of a specific GAGA factor/DNA complex reveals a modular binding mode, *Nature Struct. Biol.* **4,** 122–132 (1997).